科学通报 2026 年 第 71 卷 第 21 期: 5142 ~ 5150
量子信息与量子计算中的前沿交叉问题专题 论 文
《中国科学》杂志社 SCIENCE CHINA PRESS

非厄米系统中的非阿贝尔绝热演化与绝热捷径理论研究

周子涵, 王昕, 刘昊迪*, 衣学喜*

东北师范大学物理学院量子科学中心, 长春 130024
* 联系人, E-mail: liuhd100@nenu.edu.cn; yixx@nenu.edu.cn

2025-12-20 收稿, 2026-03-24 修回, 2026-03-25 接受, 2026-03-26 网络版发表
国家自然科学基金(12575011, 12575010)和吉林省科技发展计划(20240101321JC)资助

摘要 本文以具有非互易耦合的三脚架系统为研究对象, 系统探讨了非厄米系统中的非阿贝尔绝热演化、几何相位及其绝热捷径实现. 我们首先建立了赝厄米哈密顿量下的非阿贝尔绝热演化理论框架, 并通过数值方法求解了双正交本征态的演化过程. 研究发现, 系统非简并本征态上的布居数在绝热过程中强烈依赖于非厄米参数和初始态的选择. 而对于简并子空间中的非阿贝尔绝热演化, 其布居数和相位呈现类似厄米体系的特性; 也就是说, 非厄米性对非简并本征态布居有较大影响, 而不会影响简并本征态. 基于这些发现, 我们进一步推广了适用于该系统的绝热捷径方案并用数值模拟加以验证, 该方案在保持简并子空间内厄米特性的同时, 实现了演化速度的有效提升. 本文的研究不仅拓展了非阿贝尔绝热捷径在非厄米系统中的适用性, 也为发展非厄米量子调控技术提供了新的理论工具.

关键词 非厄米系统, 非阿贝尔绝热演化, 几何相位, 绝热捷径

自Berry于1984年提出几何相位(Berry相位)[1~3]以来, 量子系统在绝热演化过程中所获得的几何效应便成为量子力学中的核心课题之一. 几何相位的提出揭示了哈密顿量参数空间的拓扑与几何结构对量子态演化的深刻影响[4~9], 并迅速推动了量子霍尔效应[10]、分子动力学[11]、绝热捷径技术[12]等诸多领域的发展. 随后, Wilczek和Zee将几何相位推广至简并能级体系, 提出了非阿贝尔几何相位(Wilczek–Zee相位, WZ相位)[4], 使得量子系统在演化过程中不仅积累阿贝尔相因子, 还可获得具有非互易性的非阿贝尔矩阵相因子. 这一突破为非阿贝尔规范场、量子计算与量子控制[6,13~19]的研究提供了重要的理论基石.

然而, 传统的绝热过程要求系统在足够缓慢的演化下始终保持在本征态上, 这在实际物理系统中往往要求很长的演化时间才能实现, 因此容易受到退相干与噪声的影响[20~24]. 为克服这一困难, 近年来“绝热捷径”(shortcuts to adiabaticity, STA)理论得到了快速发展[25,26]. 该理论通过引入额外控制场或构造有效哈密顿量[2,27~29], 使有限时间内的动力学演化能够精确再现缓慢绝热过程的结果. 特别是Berry提出的反向透热补偿驱动(counterdiabatic driving, CD)方法[30~33], 通过消除非绝热跃迁, 实现了对量子态的快速、精确操控. 此类方案已在二能级与多能级系统的量子计算、量子信息处理等场景中展示出广泛应用前景.

近年来, 在研究几何相和量子绝热捷径等几何效应时, 人们将目光逐渐转向了非厄米量子系统. 在开放量子系统、增益-耗散动力学及拓扑物理等背景下[34,35], 非厄米哈密顿量提供了刻画非保守过程的有效工具. 尤其是PT对称与赝厄米系统在特定条件下能够保持实能谱, 从而使得几何相与绝热演化的讨论得以延伸至非厄米框架[36~53]. 更为重要的是, 非厄米系统的本征态通常需要采用双正交规范条件, 其几何相

引用格式: 周子涵, 王昕, 刘昊迪, 等. 非厄米系统中的非阿贝尔绝热演化与绝热捷径理论研究. 科学通报, 2026, 71: 5142–5150
Zhou Z-H, Wang X, Liu H-D, et al. Non-Abelian adiabatic evolution and shortcuts to adiabaticity in non-Hermitian systems (in Chinese). Chin Sci Bull, 2026, 71: 5142–5150, doi: 10.1360/CSB-2025-5932

© 2026《中国科学》杂志社

和绝热条件与传统厄米情形存在本质差异. 这导致非厄米系统中的Berry相位、WZ相位及其对应的几何效应展现出新的特征, 例如能谱中的异常点(exceptional points, EPs)[54,55]及其相关的拓扑相变和动力学临界现象. 在容错量子计算领域, 非厄米系统的简并暗态子空间可作为免受噪声干扰的量子信息编码空间. 该子空间内绝热演化积累的非阿贝尔几何相位天然地抵抗特定类型的控制误差, 为实现结合拓扑保护与非厄米调控灵活性的几何量子计算提供了新途径[56]. 在上述背景下, 非厄米系统中的绝热捷径方案也取得了重要进展. Torosov等人通过引入平衡的增益-损耗项实现了非厄米STIRAP的绝热捷径[57], Song等人进一步将反向透热驱动推广到赝厄米和反赝厄米系统, 给出了自归一化本征态的条件[58]. 上述这些研究为在非厄米系统中实现快速、鲁棒的量子操控奠定了基础.

上述研究集中在无能级简并的非厄米系统中实现绝热捷径方案. 由此, 本文重点研究以下问题: 在具有简并的非厄米系统中, 其简并子空间内的非阿贝尔绝热演化会展现出哪些区别于厄米情况的特性? 非厄米性会对非阿贝尔绝热演化产生什么影响? 以及如何找到有效的绝热捷径方案, 可以实现对非厄米非阿贝尔绝热演化过程的加速调控? 通过一个具有非互易耦合的三脚架系统, 本文开展上述问题的研究. 首先, 我们介绍了非互易耦合的三脚架模型, 及其非厄米本征问题和赝厄米特性; 其次, 通过引入新的研究非厄米简并子空间演化的纯右态方法, 我们得到了类似于厄米情况的非厄米非阿贝尔几何相位定义; 然后, 通过数值模拟, 展示了系统随具体参数进行绝热演化的过程, 讨论了非厄米性对非简并本征态布居以及简并量子态布居和几何相位的影响. 在此基础上, 进一步提出了相应的非厄米非阿贝尔绝热捷径方案, 并通过数值模拟证明了其对非厄米系统中阿贝尔和非阿贝尔绝热演化的加速效果.

1 模型与哈密顿量

考虑一个非厄米三脚架系统[59], 该系统可通过三对非互易激光与一个多能级原子相互作用实现, 如图1所示. 在相互作用绘景中, 该三脚架系统的哈密顿量表示为

$$H=\hbar\begin{pmatrix}0 & \Omega_1 & \Omega_2 & \Omega_3\\ \Omega_1' & 0 & 0 & 0\\ \Omega_2' & 0 & 0 & 0\\ \Omega_3' & 0 & 0 & 0\end{pmatrix}, \tag{1}$$

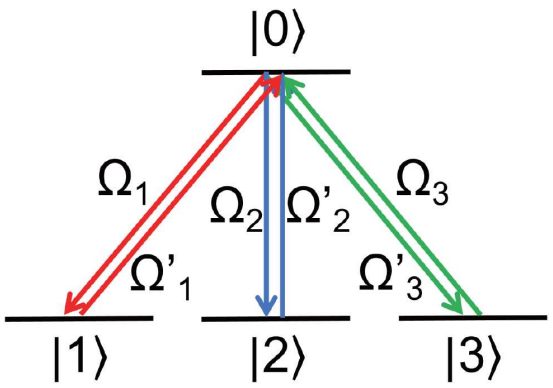


图 1 (网络版彩色)非互易三脚架系统的示意图. 此系统表示经典光场与一个四能级原子的相互作用. 经典光场与原子之间的耦合强度, 即拉比频率, 为Ω_μ和Ω_μ'(μ = 1, 2, 3)

Figure 1 (Color online) Schematic diagram of a non-reciprocal tripod system. This system represents the interaction between a classical light field and a four-level atom. The coupling strength between the classical light field and atoms, i.e., the Rabi frequency, is Ω_μ and Ω_μ' (μ = 1, 2, 3)

其中, 基底为$\{|0\rangle,|1\rangle,|2\rangle,|3\rangle\}$, 非互易的Rabi频率

$$\boldsymbol{\Omega}_a=\{\Omega_1,\Omega_2,\Omega_3\},$$
$$\Omega_1=\Omega_a\sin\gamma\cos\beta e^{i\alpha},$$
$$\Omega_2=\Omega_a\sin\gamma\sin\beta e^{i\alpha},$$
$$\Omega_3=\Omega_a\cos\gamma\ (\Omega_a=\sqrt{|\Omega_1|^2+|\Omega_2|^2+|\Omega_3|^2}),$$

以及

$$\boldsymbol{\Omega}_b=\{\Omega_1',\Omega_2',\Omega_3'\},$$
$$\Omega_1'=\Omega_b\sin\gamma'\cos\beta' e^{-i\alpha'},$$
$$\Omega_2'=\Omega_b\sin\gamma'\sin\beta' e^{-i\alpha'},$$
$$\Omega_3'=\Omega_b\cos\gamma'(\Omega_b=\sqrt{|\Omega_1'|^2+|\Omega_2'|^2+|\Omega_3'|^2}),$$

其中参数$\alpha,\beta,\gamma,\alpha',\beta',\gamma'$均为含时参数. 该哈密顿量的本征值与双正交基$\{|\psi_{0,\pm}^l(t)\rangle,|\psi_{0,\pm}^r(t)\rangle\}$为

$$E_{0,\pm}=0,\pm\hbar\Omega, \tag{2}$$
$$|\psi_{01}^r\rangle=\sin\beta|1\rangle-\cos\beta|2\rangle, \tag{3}$$
$$|\psi_{01}^l\rangle=\sin\beta'|1\rangle-\cos\beta'|2\rangle, \tag{4}$$
$$|\psi_{02}^r\rangle=\cos\gamma\cos\beta|1\rangle+\cos\gamma\sin\beta|2\rangle-\sin\gamma e^{i\alpha}|3\rangle, \tag{5}$$
$$|\psi_{02}^l\rangle=\cos\gamma'\cos\beta'|1\rangle+\cos\gamma'\sin\beta'|2\rangle-\sin\gamma' e^{i\alpha'}|3\rangle, \tag{6}$$
$$|\psi_{\pm}^r\rangle=\frac{\Omega_b}{\sqrt{2}\Omega}(\pm\frac{\Omega}{\Omega_b}|0\rangle+\sin\gamma'\cos\beta' e^{-i\alpha'}|1\rangle +\sin\gamma'\sin\beta e^{-i\alpha'}|2\rangle+\cos\gamma'|3\rangle), \tag{7}$$
$$|\psi_{\pm}^l\rangle\models\frac{\Omega_a}{\sqrt{2}\Omega}(\pm\frac{\Omega}{\Omega_a}|0\rangle+\sin\gamma\cos\beta e^{-i\alpha}|1\rangle +\sin\gamma\sin\beta e^{-i\alpha}|2\rangle+\cos\gamma|3\rangle), \tag{8}$$

其中,

$$\Omega = \sqrt{\boldsymbol{\Omega}_a \cdot \boldsymbol{\Omega}_b} = \Omega_m \sqrt{\cos\gamma\cos\gamma' + \sin\gamma\sin\gamma'\cos(\beta-\beta')\mathrm{e}^{\mathrm{i}(\alpha-\alpha')}},$$

平均频率$\Omega_m = \sqrt{\Omega_a\Omega_b}$; 相应地, 非互易参数可定义为$\Delta = \sqrt{\Omega_a/\Omega_b}$.

值得一提的是, 当$\alpha = \alpha'$时, 该哈密顿量H是一个η赝厄米哈密顿量[39~42], 满足如下关系:

$$H^\dagger = \eta H \eta^{-1}, \tag{9}$$

$$\eta = \begin{pmatrix} 1 & 0 & 0 & 0 \\ 0 & \Omega_1^*/\Omega_1^{'} & 0 & 0 \\ 0 & 0 & \Omega_2^*/\Omega_2^{'} & 0 \\ 0 & 0 & 0 & \Omega_3^*/\Omega_3^{'} \end{pmatrix}, \tag{10}$$

左右本征态满足如下关系:

$$\left|\psi_\pm^l(t)\right\rangle = \eta\left|\psi_\pm^{*r}(t)\right\rangle, \tag{11}$$

$$\begin{aligned} \boldsymbol{u}_a &= (\sin\gamma\cos\beta, \sin\gamma\sin\beta, \cos\gamma), \\ \boldsymbol{u}_b &= (\sin\gamma^{'}\cos\beta^{'}, \sin\gamma^{'}\sin\beta^{'}, \cos\gamma^{'}), \end{aligned} \tag{12}$$

之间的距离$d_{ab} = \sqrt{2-2\boldsymbol{u}_a\cdot\boldsymbol{u}_b}$决定: ① 实能谱情况: $d_{ab} < \sqrt{2}$; ② EPs: $d_{ab} = \sqrt{2}$; ③ 虚能谱情况: $d_{ab} > \sqrt{2}$.

2 非厄米简并子空间与非阿贝尔几何相位

在非厄米系统中, 如果系统哈密顿量满足能量本征方程

$$H\left|\psi_{nk}^r\right\rangle = E_n\left|\psi_{nk}^r\right\rangle, \tag{13}$$

一般来说, 系统能量本征值E_n相应的f_n重简并本征态$|\psi_{nk}\rangle(k = 1,2,3,\ldots f_n$标记简并)之间并不满足正交归一完备关系. 只有引入哈密顿量厄米共轭的能量本征方程

$$H^\dagger\left|\psi_{nk}^l\right\rangle = E_n^*\left|\psi_{nk}^l\right\rangle, \tag{14}$$

以及左本征态, 才能由双正交基$\left\{|\psi_n^l\rangle\right\}$和$\left\{|\psi_n^r\rangle\right\}$构成系统正交归一和完备关系[46]

$$\left\langle\psi_{mj}^l|\psi_{nk}^r\right\rangle = \delta_{mn}\delta_{jk}, \sum_n\sum_{k=1}^{f_n}\left|\psi_{nk}^r\right\rangle\left\langle\psi_{nk}^l\right| = I, \tag{15}$$

其中, I为单位矩阵. 对于不同能级之间的能量本征态, 左右本征态间的正交归一性是显而易见的, 如$\left\langle\psi_\pm^l|\psi_\pm^r\right\rangle = 1$, $\left\langle\psi_\pm^l|\psi_\mp^r\right\rangle = 0$. 然而, 对于简并子空间来说, 即使哈密顿量是厄米的, 其简并量子态间一般也不满足正交归一, 可以通过进行线性叠加使其满足正交归一性. 对于非厄米哈密顿量来说, 这一简并态选取的任意性, 一方面可以通过线性叠加, 使得简并子空间内的左右量子态间也满足双正交基的正交归一性; 而另一种选择则可以通过线性叠加, 使得简并右本征态自身满足正交归一性, 如

$$\left\langle\psi_{0j}^l|\psi_{0k}^l\right\rangle = \left\langle\psi_{0j}^r|\psi_{0k}^r\right\rangle = \delta_{jk}(j,k = 1,2), \tag{16}$$

这样一来, 系统零能级简并子空间的本征态却表现出与厄米系统相似的性质. 更有趣的是, 在这一选择下, 所有简并子空间中的量子态只依赖于Rabi频率$\boldsymbol{\Omega}_a$, 而所有非简并右能量本征态则恰恰相反, 只依赖于非互易Rabi频率$\boldsymbol{\Omega}_b$和能量本征值$E_{0,\pm}$. 由于简并子空间中基矢选取有效"屏蔽"了非厄米性对该子空间的影响, 使得我们可以利用非厄米简并子空间中的绝热演化得到与厄米系统相类似的非阿贝尔几何相位及其绝热捷径方案. 需要强调的是, 简并子空间内右本征态的正交归一性并非人为施加的数学条件, 只是子空间基矢的选择. 若初始时刻系统简并子空间内状态选择右态正交基张成, 则在绝热演化过程中, 系统将始终位于该子空间内, 且右态之间的正交归一关系保持不变. 反之, 如果初态选取双正交基张成的简并子空间, 则绝热演化过程中双正交归一关系保持不变.

下面我们考虑简并子空间中, 系统随参数$\boldsymbol{X} = (\alpha,\beta,\gamma,\alpha',\beta',\gamma')$的绝热演化. 其瞬时能量本征方程由下式决定

$$H(\boldsymbol{X})\left|\psi_{0k}^r(\boldsymbol{X})\right\rangle = E_0\left|\psi_{0k}^r(\boldsymbol{X})\right\rangle, \tag{17}$$

其中, $k = 1,2$. 如果考虑初态

$$\left|\psi_0\right\rangle = \sum_{k=1}^{2} C_{0k}(\boldsymbol{X}_0)\left|\psi_{0k}^r(\boldsymbol{X}_0)\right\rangle, \tag{18}$$

其中, $\boldsymbol{X}_0 = (\alpha_0,\beta_0,\gamma_0,\alpha_0^{'},\beta_0^{'},\gamma_0^{'})$. 对于包含简并子空间系统的绝热演化, 其由薛定谔方程驱动的态可以写为[4]

$$|\phi_n(\boldsymbol{X})\rangle = \sum_j C_{nj}(\boldsymbol{X}_0)\mathrm{e}^{-\frac{\mathrm{i}}{\hbar}\int_0^t E_n(\boldsymbol{X})\mathrm{d}\tau}\sum_{k=1}^{N} U_{jk}^n|\psi_{nk}^r(\boldsymbol{X})\rangle, \tag{19}$$

其中, $U_{jk}^n = \mathcal{P}\mathrm{e}^{\mathrm{i}\int_c A_{jk}^n(\boldsymbol{X})\cdot\mathrm{d}\boldsymbol{X}}$是由路径序积分给出的WZ几何相位因子, $n = 0,\pm$. 而非阿贝尔几何势$A^n(\boldsymbol{X})$的矩阵

元$A^{n}_{jk}(\boldsymbol{X})$由于简并子空间中右态自身的正交归一性, 可写为只依赖于右态的形式, 即

$$A^{n}_{jk}(\boldsymbol{X}) = \mathrm{i}\left\langle \psi^{r}_{nj}(\boldsymbol{X})|\partial_{X}\psi^{r}_{nk}(\boldsymbol{X})\right\rangle, \tag{20}$$

是非阿贝尔几何规势A^{n}的矩阵元.

考虑赝厄米情况$\alpha=\alpha'$, 简并零能本征态$\left|\psi^{r}_{0k}(\boldsymbol{X})\right\rangle$相应非阿贝尔几何势为

$$A^{0}(\boldsymbol{X}) = \mathrm{i}\begin{pmatrix} 0 & -\cos\gamma \\ \cos\gamma & 0 \end{pmatrix}\hat{\boldsymbol{e}}_{\beta}+\begin{pmatrix} 0 & 0 \\ 0 & -\sin^{2}\gamma \end{pmatrix}\hat{\boldsymbol{e}}_{\alpha}. \tag{21}$$

而对于非简并能级$E_{\pm}$, 式(19)退化为非简并形式

$$|\phi_{\pm}(\boldsymbol{X})\rangle = \mathrm{e}^{-\frac{\mathrm{i}}{\hbar}\int_{0}^{t}E_{\pm}(\boldsymbol{X})\mathrm{d}\tau+\mathrm{i}\int_{c}A^{\pm}(\boldsymbol{X})\cdot\mathrm{d}\boldsymbol{X}}|\psi^{r}_{\pm}(\boldsymbol{X})\rangle, \tag{22}$$

其中, $\mathrm{i}\int_{c}A^{\pm}(\boldsymbol{X})\cdot\mathrm{d}\boldsymbol{X}$为非简并本征态绝热演化过程中累积的非厄米几何相. 阿贝尔几何势$A^{\pm}(\boldsymbol{X})$由非简并左右本征态共同决定, 即

$$\begin{aligned} A^{\pm}(\boldsymbol{X}) &= \mathrm{i}\left\langle \psi^{l}_{\pm}(\boldsymbol{X})|\partial_{X}\psi^{r}_{\pm}(\boldsymbol{X})\right\rangle\cdot\mathrm{d}\boldsymbol{X} \\ &= \mathrm{i}\frac{\boldsymbol{u}_{a}\cdot\partial_{X}\boldsymbol{u}_{b}}{\boldsymbol{u}_{a}\cdot\boldsymbol{u}_{b}}+\frac{\Omega_{\alpha}\Omega_{\beta}}{2\Omega^{2}}\sin\gamma\sin\gamma'\cos(\beta-\beta')\hat{\boldsymbol{e}}_{\alpha}. \end{aligned} \tag{23}$$

由此可见, 尽管非简并能级的几何相位不再为实数, 且由非互易Rabi频率$\boldsymbol{\Omega}_{a}$和$\boldsymbol{\Omega}_{b}$共同决定, 而简并子空间中的WZ几何相因子仍为实, 且只由简并子空间的右本征态决定, 也就是说简并子空间中两个正交本征态上的总布居数守恒. 这为我们在非厄米系统中实现非阿贝尔几何相因子提供了一个天然的机制. 下面我们将通过具体的数值模拟来展示, 如何通过绝热演化以及绝热捷径技术实现这一理论结果.

3 非阿贝尔绝热演化及其绝热捷径

为了更直观地展示系统的非阿贝尔绝热演化过程和非互易激光带来的非厄米效应, 我们将参数选取为

$$\begin{aligned} &\alpha = 0, \\ &\beta' = \beta = \pi-\frac{\pi}{2}\cos\frac{\pi t}{\tau}, \\ &\gamma' = \gamma = \frac{\pi}{2}-\frac{\pi}{4}\sin\frac{\pi t}{\tau}, \end{aligned} \tag{24}$$

于是, 由式(21)和(23)可知, 对于系统任意量子态

$$\begin{aligned} |\psi(\boldsymbol{X})\rangle = {} & C_{01}(\boldsymbol{X})\left|\psi^{r}_{01}(\boldsymbol{X})\right\rangle+C_{02}(\boldsymbol{X})\left|\psi^{r}_{02}(\boldsymbol{X})\right\rangle \\ & +C_{+}(\boldsymbol{X})|\psi^{r}_{+}(\boldsymbol{X})\rangle+C_{-}(\boldsymbol{X})|\psi^{r}_{-}(\boldsymbol{X})\rangle, \end{aligned} \tag{25}$$

在随参数绝热演化下, 其本征态上的布居数

$$P_{0k}(\boldsymbol{X}) = \left|C_{0k}(\boldsymbol{X})\right|^{2} = \left|\left\langle \psi^{r}_{0k}(\boldsymbol{X})|\psi(\boldsymbol{X})\right\rangle\right|^{2}$$

$$P_{\pm}(\boldsymbol{X}) = |C_{\pm}(\boldsymbol{X})|^{2} = \left|\left\langle \psi^{l}_{\pm}(\boldsymbol{X})|\psi(\boldsymbol{X})\right\rangle\right|^{2}$$

和相位

$$\theta_{0k}(\boldsymbol{X}) = \arg\left(\left\langle \psi^{r}_{0k}(\boldsymbol{X})|\psi(\boldsymbol{X})\right\rangle\right),$$

$$\theta_{\pm}(\boldsymbol{X}) = \arg\left(\left\langle \psi^{l}_{\pm}(\boldsymbol{X})|\psi(\boldsymbol{X})\right\rangle\right)$$

的动力学演化为

$$\dot{P}_{+} = \dot{P}_{-} = 0, \tag{26}$$

$$\dot{P}_{01} = -\dot{P}_{02} = 2\sqrt{P_{01}P_{02}}\cos(\theta_{01}-\theta_{02})\cos\gamma\dot{\beta}, \tag{27}$$

$$\dot{\theta}_{01} = \sqrt{\frac{P_{02}}{P_{01}}}\sin(\theta_{01}-\theta_{02})\cos\gamma\dot{\beta}, \tag{28}$$

$$\dot{\theta}_{02} = -\sin^{2}\eta\dot{\alpha}+\sqrt{\frac{P_{01}}{P_{02}}}\sin(\theta_{01}-\theta_{02})\cos\gamma\dot{\beta}, \tag{29}$$

$$\dot{\theta}_{+} = -\Omega+\frac{1}{2}\sin^{2}2\gamma\dot{\alpha}, \tag{30}$$

$$\dot{\theta}_{-} = \Omega+\frac{1}{2}\sin^{2}2\gamma\dot{\alpha}. \tag{31}$$

由此可见, 在非厄米系统绝热演化过程中, 每个能级上的布居数是不变的, 而对于简并子空间, 尽管布居数总和不变, 两个简并本征态的布居数是随时间变化的. 通过选取$|\psi_{0}\rangle = \frac{1}{2}\left(|0\rangle+|1\rangle+|2\rangle+\mathrm{e}^{\mathrm{i}\phi}|3\rangle\right)$为初态并取$\alpha$=0, 严格数值求解非厄米哈密顿量$H$满足的薛定谔方程, 我们在图2中说明非厄米绝热和非绝热演化对布居数及简并子空间几何相位的效应.

在图2(a)和(b)所描述的非绝热演化过程(T=5τ)中, 无论对于厄米情况(Δ=1)还是非厄米情况($\Delta=\sqrt{2}$), 本征态上的布居数都产生了较大波动, 尤其是非厄米情况下还出现了总布居数不守恒且大于1的情况. 而图2(c)和(d)所示的绝热情况(T=300τ)下, 非简并子空间的布居数P_{+}和P_{-}以及简并子空间的总布居数P_{01}+P_{02}几乎不随时间变化. 而不同非厄米性($\Delta=\sqrt{2}, 1/\sqrt{2}$)对非简并子空间的布居数有着显著的影响. 与之相应地, 简并子空间的布居数演化完全不受非厄米性的影响, 这充分证明了我们在简并子空间构建与厄米情况类似的、只依赖于右态的正交归一关系是正确的. 图2(e)和(f)则展示了非简并子空间中本征态上相位θ_{01}和θ_{02}的变化. 在初始相位差为0的情况下, 绝热演化所累积的相位呈现出了整数π之间的跳变; 而在初始相位差为$-\pi/4$的情况下, 则呈现出了线性变化, 这为构建依赖于非阿贝尔几何相位的几何量子计算方案提出了一种有趣的机制.

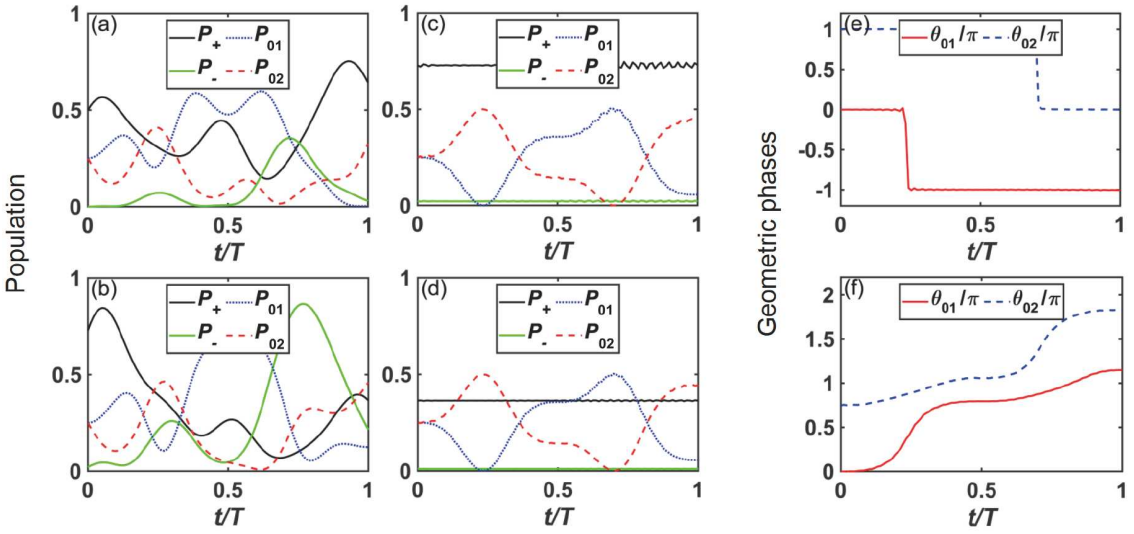


图 2 (网络版彩色)系统本征态上布居数P_{0k}、$P_{\pm}$以及简并子空间本征态上相位θ_{0k}随参数变化一周期的时间演化. 参数选取为: (a) $\tau = T/5$, $\Delta = 1$, $\phi = 0$; (b) $\tau = T/5$, $\Delta = \sqrt{2}$, $\phi = 0$; (c) $\tau = T/300$, $\Delta = \sqrt{2}$,$\phi = 0$; (d) $\tau = T/300$, $\Delta = 1/\sqrt{2}$, $\phi = 0$; (e) $\tau = T/300$, $\Delta = \sqrt{2}$, $\phi = 0$; (f)$\tau = T/300$, $\Delta = \sqrt{2}$, $\phi = -\pi/4$. 系统初态为$|\psi_0\rangle = \frac{1}{2}(|0\rangle + |1\rangle + |2\rangle + e^{i\phi}|3\rangle)$

Figure 2 (Color online) The evolution of the populations P_{0k} and $P_{\pm}$ on the energy eigenstates and the phasesθ_{0k} for the degenerate eigenstates as the parameters evolving in one period. The parameters are chosen as (a) $\tau = T/5$, $\Delta = 1$, $\phi = 0$; (b) $\tau = T/5$, $\Delta = \sqrt{2}$, $\phi = 0$; (c) $\tau = T/300$, $\Delta = \sqrt{2}$, $\phi = 0$; (d) $\tau = T/300$, $\Delta = 1/\sqrt{2}$, $\phi = 0$; (e) $\tau = T/300$, $\Delta = \sqrt{2}$, $\phi = 0$; (f) $\tau = T/300$, $\Delta = \sqrt{2}$, $\phi = -\pi/4$. The initial state is $|\psi_0\rangle = \frac{1}{2}(|0\rangle + |1\rangle + |2\rangle + e^{i\phi}|3\rangle)$

然而, 在将绝热演化用于实际量子信息处理和量子计算场景时, 实现绝热条件的长演化时间(T=300τ)使得量子绝热过程极易受到环境噪声和退相干的影响[3~8]. 为了解决这一问题, 下面研究如何利用非厄米绝热捷径技术来"加速"这一绝热演化过程, 使其在较短演化时间(T=5τ)内实现这一绝热演化过程. 为理解绝热捷径技术的原理, 将系统从裸基变换到绝热基表示, 此时哈密顿量变换为

$$H_a(\boldsymbol{X}) = U(\boldsymbol{X})^{-1}H(\boldsymbol{X})U(\boldsymbol{X}) - \mathrm{i}\hbar U(\boldsymbol{X})^{-1}\dot{U}(\boldsymbol{X}), \tag{32}$$

其中, $U_{nk}(\boldsymbol{X}) = \langle n \mid \psi_k(\boldsymbol{X})\rangle$. 经过简单的推导可得:

$$[U(\boldsymbol{X})^{-1}\dot{U}(\boldsymbol{X})]_{kq} = \left\langle \psi_k^l(\boldsymbol{X}) \mid \dot{\psi}_q^r(\boldsymbol{X}) \right\rangle. \tag{33}$$

在$\beta = \beta', \gamma = \gamma', \alpha = \alpha' = 0$时, 有

$$H_a(\boldsymbol{X}) = \hbar \begin{pmatrix} \Omega & -\frac{\mathrm{i}\Delta\sin\gamma\dot{\beta}}{\sqrt{2}} & \frac{\mathrm{i}\Delta\dot{\gamma}}{\sqrt{2}} & 0 \\ \frac{\mathrm{i}\sin\gamma\dot{\beta}}{\sqrt{2}\Delta} & 0 & \mathrm{i}\cos\gamma\dot{\beta} & \frac{\mathrm{i}\sin\gamma\dot{\beta}}{\sqrt{2}\Delta} \\ \frac{-\mathrm{i}\dot{\gamma}}{\sqrt{2}\Delta} & -\mathrm{i}\cos\gamma\dot{\beta} & 0 & \frac{-\mathrm{i}\dot{\gamma}}{\sqrt{2}\Delta} \\ 0 & -\frac{\mathrm{i}\Delta\sin\gamma\dot{\beta}}{\sqrt{2}} & \frac{\mathrm{i}\Delta\dot{\gamma}}{\sqrt{2}} & -\Omega \end{pmatrix}. \tag{34}$$

作为比较典型的绝热捷径方案, 无跃迁量子驱动技术或反向透热驱动技术[30~33]就是通过引入新的哈密顿量, 将$H_a(\boldsymbol{X})$中除非阿贝尔相之外的代表能级间跃迁的非对角项抵消, 从而实现加速绝热过程. 最后, 再将引入的附加哈密顿量变换到裸基, 讨论其相应的实现方案.

根据非阿贝尔系统的反向透热补偿驱动理论(counterdiabatic driving)[60], 我们构建了相应的绝热捷径方案. 与传统方案不同, 我们在简并子空间内采用的是纯右态构建的正交归一关系. 由此, 修正后的总哈密顿量H_{CD}满足如下关系:

$$\begin{aligned} H_{\mathrm{CD}}(\boldsymbol{X}) &= H(\boldsymbol{X}) + H_{\mathrm{I}}(\boldsymbol{X}), \\ H(\boldsymbol{X}) &= \sum_n \left|\psi_n^r(\boldsymbol{X})\right\rangle E_n(\boldsymbol{X}) \left\langle\psi_n^l(\boldsymbol{X})\right|, \\ H_{\mathrm{I}}(\boldsymbol{X}) &\equiv \mathrm{i}\hbar\Bigg[\sum_{\pm}\left|\partial_t\psi_{\pm}^r(\boldsymbol{X})\right\rangle\left\langle\psi_{\pm}^l(\boldsymbol{X})\right| \\ &\quad + \sum_{k=1}^{2}\left|\partial_t\psi_{0k}^r(\boldsymbol{X})\right\rangle\left\langle\psi_{0k}^r(\boldsymbol{X})\right| \\ &\quad - \sum_{\pm}\left\langle\psi_{\pm}^l(\boldsymbol{X}) \mid \partial_t\psi_{\pm}^r(\boldsymbol{X})\right\rangle\left|\psi_{\pm}^r(\boldsymbol{X})\right\rangle\left\langle\psi_{\pm}^l(\boldsymbol{X})\right| \\ &\quad - \sum_{j,k=1}^{2}\left\langle\psi_{0j}^r(\boldsymbol{X}) \mid \partial_t\psi_{0k}^r(\boldsymbol{X})\right\rangle\left|\psi_{0j}^r(\boldsymbol{X})\right\rangle\left\langle\psi_{0k}^r(\boldsymbol{X})\right|\Bigg], \end{aligned} \tag{35}$$

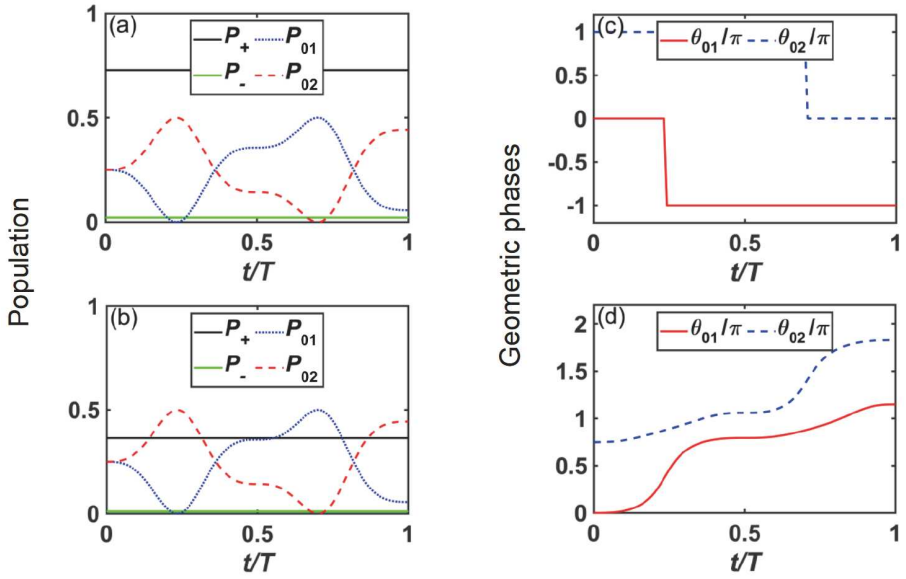


图 3 (网络版彩色)系统本征态上布居数P_{0k}、$P_{\pm}$以及简并子空间本征态上相位θ_{0k}在哈密顿量$H_{\mathrm{CD}}(\boldsymbol{X})$驱动下随参数变化一周期的时间演化. 参数选取为: (a) $\tau=T/5$, $\Delta=\sqrt{2}$, $\phi=0$; (b) $\tau=T/5$, $\Delta=1/\sqrt{2}$, $\phi=0$; (c) $\tau=T/5$, $\Delta=\sqrt{2}$, $\phi=0$; (d) $\tau=T/5$, $\Delta=\sqrt{2}$, $\phi=-\pi/4$. 系统初态为$|\psi_0\rangle=\left(\frac{1}{2}|0\rangle+|1\rangle+|2\rangle+\mathrm{e}^{\mathrm{i}\phi}|3\rangle\right)$

Figure 3 (Color online) The evolution of the populations P_{0k} and $P_{\pm}$ on the energy eigenstates and the phases θ_{0k} for the degenerate eigenstates as the parameters evolving in one period driven by the Hamiltonian $H_{\mathrm{CD}}(\boldsymbol{X})$. The parameters are chosen as: (a) $\tau=T/5$, $\Delta=\sqrt{2}$, $\phi=0$; (b) $\tau=T/5$, $\Delta=1/\sqrt{2}$, $\phi=0$; (c) $\tau=T/5$, $\Delta=\sqrt{2}$, $\phi=0$; (d) $\tau=T/5$, $\Delta=\sqrt{2}$, $\phi=-\pi/4$. The initial state is $|\psi_0\rangle=\left(\frac{1}{2}|0\rangle+|1\rangle+|2\rangle+\mathrm{e}^{\mathrm{i}\phi}|3\rangle\right)$

其中, $H(\boldsymbol{X})$是系统原始哈密顿量, $H_{\mathrm{I}}(\boldsymbol{X})$是反向透热补偿驱动哈密顿量, $H_{\mathrm{I}}(\boldsymbol{X})$中的前两项抵消了能量跃迁项, 第二部分产生了WZ相(即非阿贝尔几何相). 因此, 结合式(2)~(8), 可以得到在$\beta=\beta'$, $\gamma=\gamma'$, $\alpha=\alpha'$时完整的绝热捷径哈密顿量表达式:

$$H_{\mathrm{CD}}=\hbar\begin{pmatrix}-\frac{1}{2}\sin^2\eta\dot{\alpha} & \Omega_1 & \Omega_2 & \Omega_3\\ \Omega_1' & D & C^* & B_+^*\\ \Omega_2' & C & F & B_-^*\\ \Omega_3' & B_+ & B_- & -\frac{3}{8}\sin^2 2\eta\dot{\alpha}\end{pmatrix}. \tag{36}$$

其中,

$$\begin{aligned}
&B_{\pm}=\frac{1}{16}\cos\beta(2\sin 2\gamma+3\sin 4\gamma)\mathrm{e}^{\mathrm{i}\alpha}\dot{\alpha}\\
&-\mathrm{i}\cos\beta\mathrm{e}^{\mathrm{i}\alpha}\dot{\gamma}\pm\frac{1}{2}\mathrm{i}\sin\beta\sin 2\gamma\mathrm{e}^{\mathrm{i}\alpha}\dot{\beta},\\
&C=\frac{1}{8}\sin 2\beta\sin^2\gamma(5+3\cos 2\gamma)\dot{\alpha}+\mathrm{i}\sin^2\gamma\dot{\beta},\\
&D=\frac{1}{4}\cos^2\beta\sin^2\gamma(5+3\cos 2\gamma)\dot{\alpha},\\
&F=\frac{1}{4}\sin^2\beta\sin^2\gamma(5+3\cos 2\gamma)\dot{\alpha}.
\end{aligned} \tag{37}$$

若取α=0, 则可进一步化简为

$$H_{\mathrm{CD}}=\hbar\begin{pmatrix}0 & \Omega_1 & \Omega_2 & \Omega_3\\ \Omega_1' & 0 & P & Q\\ \Omega_2' & -P & 0 & R\\ \Omega_3' & -Q & -R & 0\end{pmatrix}, \tag{38}$$

$$\begin{aligned}
&P=-\mathrm{i}\sin^2\gamma\dot{\beta},\\
&Q=\mathrm{i}\cos\beta\dot{\gamma}-\mathrm{i}\cos\gamma sin\beta\sin\gamma\dot{\beta},\\
&R=\mathrm{i}\sin\beta\dot{\gamma}+\mathrm{i}\cos\beta\sin\gamma\cos\gamma\dot{\beta},
\end{aligned}$$

在这个新的哈密顿量的驱动下, 系统可以不依赖于绝热条件, 即在快速演化的条件下, 也可以保证系统一直在初始的能量本征空间内演化, 达到绝热图2(c)~(f)的演化效果.

下面, 我们通过数值求解哈密顿量H_{CD}满足的薛定谔方程来验证绝热捷径方案的有效性, 并将结果展示在图3中. 由图3(a)和(b)可以看出, 在H_{CD}驱动的短时演化(T=5τ)情况下, 布居数P_+和P_-以及简并子空间的总布居数P_{01}+P_{02}严格守恒, 这实现了比原始哈密顿量H驱动长时绝热演化(T=300τ)下更严格的结果(如图2(c)和(d)所示), 而原始哈密顿量在短时演化下无论总布居数还是各能级布居数都不守恒(如图2(b)所示). 此外, 非厄米性对布居数的影响也得到了体现. 相应地, 图3(c)和(d)展示

了简并量子态相位的变化, 同样也重现了原始哈密顿量的绝热演化结果(如图2(e)和(f)所示). 这说明只要在裸态|1⟩和|2⟩、|1⟩和|3⟩、|2⟩和|3⟩之间加入互易驱动, 就可以实现非厄米非阿贝尔绝热演化, 这为其应用到非厄米非阿贝尔量子信息和量子计算领域提供了新思路.

4 总结

本文系统研究了非厄米三脚架系统中的非阿贝尔绝热演化与绝热捷径理论. 通过建立赝厄米框架下的理论模型并数值求解双正交本征态的演化, 我们分别揭示了系统布居行为对非厄米参数和初始态的依赖关系: 当初始态处于简并子空间时, 系统表现出与厄米体系类似的布居守恒特性, 而对于非简并态上的布居, 则呈现出非厄米系统特有的放大或缩小效应; 改变非互易参数会导致系统总布居数随时间演化, 但简并子空间内的布居数始终保持不变, 这一现象也凸显了简并子空间在非互易系统中独特的类厄米特性. 基于这些发现, 我们成功构建了适用于该非厄米系统的绝热捷径方案. 该方案通过反向透热补偿驱动方法, 在保证了简并子空间类厄米特性的同时实现了演化过程的显著加速. 数值模拟结果表明, 应用绝热捷径技术后, 系统在快速演化过程中仍能保持各能级布居数的守恒, 验证了该方案的有效性. 本研究不仅拓展了非阿贝尔绝热捷径在非厄米系统中的适用性, 还提供了解决非厄米系统中快速绝热操控的新思路, 为将其应用于非厄米量子信息处理和量子调控技术奠定了理论基础. 值得注意的是, 本研究中发现的简并子空间类厄米特性还在容错量子计算领域具有重要的应用前景. 简并暗态子空间可作为天然的噪声免疫计算空间, 其中编码的量子信息能够免受非厄米系统固有的增益与损耗效应影响. 在该子空间内通过绝热演化积累的非阿贝尔几何相位——即Wilczek-Zee相位——天然地抵抗特定类型的控制误差, 为实现基于几何相位的全量子计算提供了理想平台. 更重要的是, 我们构建的绝热捷径方案使得这种几何量子门可以在远短于绝热条件要求的时间尺度内实现, 有效克服了退相干和噪声对长时绝热过程的影响. 这一进展为在非厄米物理系统中实现快速、鲁棒的量子门操作开辟了新途径.

参考文献

1 Pancharatnam S. Generalized theory of interference, and its applications. Proc Ind Acad Sci, 1956, 44: 247–262
2 Longuet-Higgins H C, Öpik U, Pryce M H L, et al. Studies of the Jahn-Teller effect. II. The dynamical problem. Proc R Soc A-Math Phys Eng Sci, 1958, 244: 1–16
3 Berry M V. Quantal phase factors accompanying adiabatic changes. Proc R Soc London A Math Phys Sci, 1984, 392: 45–57
4 Wilczek F, Zee A. Appearance of gauge structure in simple dynamical systems. Phys Rev Lett, 1984, 52: 2111–2114
5 Hannay J H. Angle variable holonomy in adiabatic excursion of an integrable Hamiltonian. J Phys A-Math Gen, 1985, 18: 221–230
6 Aharonov Y, Anandan J. Phase change during a cyclic quantum evolution. Phys Rev Lett, 1987, 58: 1593–1596
7 Sjöqvist E, Pati A K, Ekert A, et al. Geometric phases for mixed states in interferometry. Phys Rev Lett, 2000, 85: 2845–2849
8 Yi X X, Wang L C, Zheng T Y. Berry phase in a composite system. Phys Rev Lett, 2004, 92: 150406
9 Tong D M, Sjöqvist E, Kwek L C, et al. Kinematic approach to the mixed state geometric phase in nonunitary evolution. Phys Rev Lett, 2004, 93: 080405
10 Laughlin R B. The relationship between high-temperature superconductivity and the fractional quantum Hall effect. Science, 1988, 242: 525–533
11 Sjöqvist E, Hedström M. Noncyclic geometric phase, coherent states, and the time-dependent variational principle: application to coupled electron-nuclear dynamics. Phys Rev A, 1997, 56: 3417–3424
12 Berry M V. Transitionless quantum driving. J Phys A-Math Theor, 2009, 42: 365303
13 Unanyan R, Fleischhauer M, Shore B W, et al. Robust creation and phase-sensitive probing of superposition states via stimulated Raman adiabatic passage (STIRAP) with degenerate dark states. Optics Commun, 1998, 155: 144–154
14 Pachos J, Zanardi P, Rasetti M. Non-Abelian Berry connections for quantum computation. Phys Rev A, 1999, 61: 010305
15 Singh K, Tong D M, Basu K, et al. Geometric phases for nondegenerate and degenerate mixed states. Phys Rev A, 2003, 67: 032106
16 Gong J, Rice S A. General method for complete population transfer in degenerate systems. Phys Rev A, 2004, 69: 063410
17 Takahashi K. Transitionless quantum driving for spin systems. Phys Rev E, 2013, 87: 062117
18 Simeonov L S, Vitanov N V. Generation of non-Abelian geometric phases in degenerate atomic transitions. Phys Rev A, 2017, 96: 032102
19 Snizhko K, Egger R, Gefen Y. Non-Abelian Berry phase for open quantum systems: topological protection versus geometric dephasing. Phys Rev B, 2019, 100: 085303
20 Bergmann K, Theuer H, Shore B W. Coherent population transfer among quantum states of atoms and molecules. Rev Mod Phys, 1998, 70: 1003–1025

21 Král P, Thanopulos I, Shapiro M. Colloquium: Coherently controlled adiabatic passage. Rev Mod Phys, 2007, 79: 53–77
22 Wu S L, Huang X L, Li H, et al. Adiabatic evolution of decoherence-free subspaces and its shortcuts. Phys Rev A, 2017, 96: 042104
23 Vitanov N V. High-fidelity multistate stimulated Raman adiabatic passage assisted by shortcut fields. Phys Rev A, 2020, 102: 023515
24 Deng J, Wang Q, Liu Z, et al. Boosting work characteristics and overall heat-engine performance via shortcuts to adiabaticity: quantum and classical systems. Phys Rev E, 2013, 88: 062122
25 Chen X, Ruschhaupt A, Schmidt S, et al. Fast optimal frictionless atom cooling in harmonic traps: shortcut to adiabaticity. Phys Rev Lett, 2010, 104: 063002
26 Guéry-Odelin D, Ruschhaupt A, Kiely A, et al. Shortcuts to adiabaticity: concepts, methods, and applications. Rev Mod Phys, 2019, 91: 045001
27 Chen Y H, Xia Y, Wu Q C, et al. Method for constructing shortcuts to adiabaticity by a substitute of counterdiabatic driving terms. Phys Rev A, 2016, 93: 052109
28 Rigolin G, Ortiz G. Adiabatic theorem for quantum systems with spectral degeneracy. Phys Rev A, 2012, 85: 062111
29 Zhang Q. Quantum adiabatic evolution with energy degeneracy levels. Phys Rev A, 2016, 93: 012116
30 Jain S R, Pati A K. Adiabatic geometric phases and response functions. Phys Rev Lett, 1998, 80: 650–653
31 González G, Leuenberger M N. Berry-phase blockade in single-molecule magnets. Phys Rev Lett, 2007, 98: 256804
32 Bruno P, Dugaev V K, Taillefumier M. Topological Hall effect and Berry phase in magnetic nanostructures. Phys Rev Lett, 2004, 93: 096806
33 Simon B. Holonomy, the quantum adiabatic theorem, and Berry's phase. Phys Rev Lett, 1983, 51: 2167–2170
34 El-Ganainy R, Makris K G, Khajavikhan M, et al. Non-Hermitian physics and PT symmetry. Nat Phys, 2018, 14: 11–19
35 Ashida Y, Gong Z, Ueda M. Non-Hermitian physics. Adv Phys, 2020, 69: 249–435
36 Miri M A, Alù A. Exceptional points in optics and photonics. Science, 2019, 363: eaar7709
37 Zhu W, Fang X, Li D, et al. Simultaneous observation of a topological edge state and exceptional point in an open and non-Hermitian acoustic system. Phys Rev Lett, 2018, 121: 124501
38 Wu Y, Liu W, Geng J, et al. Observation of parity-time symmetry breaking in a single-spin system. Science, 2019, 364: 878–880
39 Li J, Harter A K, Liu J, et al. Observation of parity-time symmetry breaking transitions in a dissipative Floquet system of ultracold atoms. Nat Commun, 2019, 10: 855
40 Xiong W, Li Z, Song Y, et al. Higher-order exceptional point in a pseudo-Hermitian cavity optomechanical system. Phys Rev A, 2021, 104: 063508
41 Xiong W, Li Z, Zhang G Q, et al. Higher-order exceptional point in a blue-detuned non-Hermitian cavity optomechanical system. Phys Rev A, 2022, 106: 033518
42 Wang X, Liu H D, Yi X X. Berry phase and quantum entanglement in a nonreciprocal composite system. Phys Rev A, 2024, 109: 062220
43 Bender C M, Boettcher S. Real spectra in non-Hermitian Hamiltonians having $\mathcal{PT}$ symmetry. Phys Rev Lett, 1998, 80: 5243–5246
44 Wong J. Results on certain non-Hermitian Hamiltonians. J Math Phys, 1967, 8: 2039–2042
45 Faisal F H M, Moloney J V. Time-dependent theory of non-Hermitian Schrödinger equation: application to multiphoton-induced ionisation decay of atoms. J Phys B-At Mol Phys, 1983, 16: 3109
46 Mostafazadeh A. Pseudo-Hermiticity versus PT symmetry: the necessary condition for the reality of the spectrum of a non-Hermitian Hamiltonian. J Math Phys, 2002, 43: 205–214
47 Mostafazadeh A. Pseudo-Hermiticity versus PT-symmetry. II. A complete characterization of non-Hermitian Hamiltonians with a real spectrum. J Math Phys, 2002, 43: 2814–2816
48 Mostafazadeh A. Pseudo-Hermiticity versus PT-symmetry III: equivalence of pseudo-Hermiticity and the presence of antilinear symmetries. J Math Phys, 2002, 43: 3944–3951
49 Mostafazadeh A. Pseudo-supersymmetric quantum mechanics and isospectral pseudo-Hermitian Hamiltonians. Nucl Phys B, 2002, 640: 419–434
50 Mostafazadeh A. Pseudo-Hermiticity for a class of nondiagonalizable Hamiltonians. J Math Phys, 2002, 43: 6343–6352
51 Mostafazadeh A. Pseudo-Hermiticity and generalized *PT*- and *CPT*-symmetries. J Math Phys, 2003, 44: 974–989
52 Mostafazadeh A. Pseudounitary operators and pseudounitary quantum dynamics. J Math Phys, 2004, 45: 932–946
53 Zhao W L. Quantization of out-of-time-ordered correlators in non-Hermitian chaotic systems. Phys Rev Res, 2022, 4: 023004
54 Minganti F, Miranowicz A, Chhajlany R W, et al. Quantum exceptional points of non-Hermitian Hamiltonians and Liouvillians: the effects of quantum jumps. Phys Rev A, 2019, 100: 062131
55 Longstaff B, Graefe E M. Nonadiabatic transitions through exceptional points in the band structure of a *PT*-symmetric lattice. Phys Rev A, 2019, 100: 052119
56 Pinske J, Teuber L, Scheel S. Holonomic gates in pseudo-Hermitian quantum systems. Phys Rev A, 2019, 100: 042316
57 Torosov B T, Della Valle G, Longhi S. Non-Hermitian shortcut to stimulated Raman adiabatic passage. Phys Rev A, 2014, 89: 063412
58 Song Y H, Wang X, Liu H D, et al. Counterdiabatic driving for pseudo- and antipseudo-Hermitian systems. J Phys A-Math Theor, 2023, 56: 015304
59 Ruseckas J, Juzeliūnas G, Öhberg P, et al. Non-Abelian gauge potentials for ultracold atoms with degenerate dark states. Phys Rev Lett, 2005, 95: 010404
60 Karzig T, Pientka F, Refael G, et al. Shortcuts to non-Abelian braiding. Phys Rev B, 2015, 91: 201102

Summary for “非厄米系统中的非阿贝尔绝热演化与绝热捷径理论研究”

Non-Abelian adiabatic evolution and shortcuts to adiabaticity in non-Hermitian systems

Zi-Han Zhou, Xin Wang, Hao-Di Liu* & Xue-Xi Yi*

Center for Quantum Sciences, School of Physics, Northeast Normal University, Changchun 130024, China
* Corresponding authors, E-mail: liuhd100@nenu.edu.cn; yixx@nenu.edu.cn

The geometric phase and its non-Abelian generalization have been fundamental concepts in quantum mechanics since Berry′s work in 1984, revealing connections between quantum evolution and the geometric structure of parameter space. While traditional adiabatic theorems guarantee that quantum systems remain in instantaneous eigenstates under sufficiently slow evolution, the required long evolution times make practical implementations vulnerable to decoherence and environmental noise. Shortcuts to adiabaticity (STA) have been developed to overcome this limitation by engineering auxiliary control fields that exactly reproduce adiabatic dynamics within finite time intervals. Meanwhile, the extension of geometric phase to non-Hermitian systems has attracted growing interest due to their natural description of open quantum systems, gain-loss dynamics, and topological phases. However, the interplay between non-Hermiticity, degenerate subspaces, and non-Abelian geometric phases remains largely unexplored, particularly regarding the possibility of accelerating non-Abelian adiabatic evolution in non-Hermitian settings.

This work investigates non-Abelian adiabatic evolution and shortcuts to adiabaticity in a four-level tripod system with nonreciprocal coupling, which serves as a paradigmatic model for studying non-Hermitian effects in quantum optics and atomic physics. We first establish a theoretical framework for non-Abelian adiabatic evolution under pseudo-Hermitian Hamiltonians, where the biorthogonal eigenbasis provides the natural description of the system′s Hilbert space structure. By carefully analyzing the orthonormality conditions within the degenerate subspace, we demonstrate that a purely right-eigenstate basis can be constructed that maintains orthonormality throughout the evolution, effectively shielding the degenerate subspace from non-Hermitian effects. This crucial observation allows us to define non-Abelian geometric phases within the degenerate subspace that remain real-valued and exhibit properties analogous to those in Hermitian systems, despite the overall non-Hermitian nature of the Hamiltonian.

Through detailed numerical simulations, we elucidate the distinct behaviors of nondegenerate and degenerate eigenstates during adiabatic evolution. For nondegenerate eigenstates, the population dynamics exhibit strong sensitivity to both the non-Hermitian parameters (characterized by Δ) and the choice of initial state, with total population conservation generally violated due to the non-unitary nature of the evolution. On the contrary, for initial states prepared within the degenerate subspace, the total population remains perfectly conserved, and the populations of individual degenerate eigenstates evolve independently of the non-Hermitian parameters. Moreover, the geometric phases accumulated within the degenerate subspace are real and depend solely on the right eigenstates, reproducing the characteristic features of non-Abelian Wilczek-Zee phases in Hermitian systems. These findings establish that degenerate subspaces in non-Hermitian systems can serve as robust platforms for realizing non-Abelian geometric manipulations that are immune to the dissipative and amplifying effects typically associated with non-Hermitian Hamiltonians.

Building on these insights, we develop a counter-diabatic driving scheme specifically tailored for non-Hermitian non-Abelian systems. Unlike conventional STA approaches that rely on Hermitian structures, our construction respects the biorthogonal nature of the eigenbasis while preserving the special properties of the degenerate subspace. The resulting shortcut Hamiltonian H_{CD} explicitly cancels nonadiabatic transitions between different eigenspaces while generating the desired non-Abelian geometric phases within the degenerate subspace. Numerical simulations demonstrate that under H_{CD} driving, the system achieves in short evolution times (T=5τ) what would otherwise require prohibitively long adiabatic evolution (T=300τ) under the original Hamiltonian. The populations of nondegenerate eigenstates remain strictly conserved, and the degenerate subspace evolution precisely reproduces the adiabatic geometric phases, confirming the effectiveness of our approach.

Our work establishes a framework for understanding and controlling non-Abelian adiabatic evolution in non-Hermitian systems, revealing the remarkable resilience of degenerate subspaces to non-Hermitian perturbations and demonstrating the feasibility of accelerating such evolution through carefully designed shortcut protocols. These results open new avenues for quantum information processing in non-Hermitian settings, particularly for geometric quantum computation schemes that leverage the topological protection of non-Abelian phases. The theoretical tools developed here may also find applications in exploring novel non-Hermitian topological phases and developing robust quantum control techniques for open quantum systems.

non-Hermitian systems, non-Abelian adiabatic evolution, geometric phase, shortcuts to adiabaticity

doi: 10.1360/CSB-2025-5932